U.S. DEPARTMENT OF ENERGY | Office of Science

DOE/SC-CM-20-003

FY 2020 Third Quarter Performance Metric: Analyze the Characteristics of the Large-Scale Environment Associated with Mesoscale Convective Systems in E3SM and Their Potential Future Changes

June 2020

DISCLAIMER

Contents

Figures

1.0 Product Definition

Mesoscale convective systems (MCSs) consist of assemblies of cumulonimbus clouds on scales of 100 km or more and produce mesoscale circulations (Houze 2004, 2018). As the largest form of deep convective storms, MCSs contribute to 30%–70% of annual and warm-season rainfall as well as over half of the extreme daily rainfall events in the U.S. east of the Rocky Mountains (Stevenson and Schumacher 2014, Feng et al. 2019, Haberlie and Ashley 2019). As part of the water cycle experiments, the Energy Exascale Earth System Model (E3SM) v1 has been configured at low (~ 100 km) and high (~ 25 km) resolution to evaluate the impacts of model resolution on simulating water cycle processes such as precipitation, snowpack, and runoff (Caldwell et al. 2019). Since MCSs contribute importantly to mean and extreme precipitation in the U.S. and many other regions around the world, understanding how well they are simulated by the model may guide future development towards more skillful modeling of convective storms and associated hydrologic impacts. The FY2020 Second Quarter Performance Metric Report documented comparisons of MCSs in the central and eastern U.S. in a high-resolution simulation produced by E3SM v1 at 25-km resolution with observations. MCSs in the simulation occur less frequently and produce less intense precipitation, resulting in a large underestimation of MCS volumetric rain-rate compared to observations. Model biases in simulating MCSs may be attributed to model limitations in parameterizing convection, clouds, and other related processes but model biases in simulating the MCS large-scale environment may also play an important role. This document summarizes analyses performed to evaluate the springtime MCS large-scale environment in the E3SM v1 high-resolution simulation, making use of a 20-year segment of the simulation with a high-frequency model output of atmospheric circulation to understand the contribution of large-scale circulation biases to modeling MCSs in the U.S. Combined with the MCS tracking used in the second quarter metric report, the analysis of large-scale environment described in this report lays the foundation for investigating how MCSs and their large-scale environment may change in the future, with implications for water availability and floods.

2.0 Product Documentation

E3SM v1 has been used to perform simulation at high resolution (HR) following the Coupled Model Intercomparison Project Phase 6 (CMIP6) HighResMIP protocol (Haarsma et al. 2016). The HR configuration features the atmosphere and land models at ~25-km grid spacing and the ocean and sea ice models at 6–18-km grid spacing. Following HighResMIP, a 100-year control simulation with time-invariant 1950 forcing has been completed. Caldwell et al. (2019) documented the model configuration and evaluation of key climatological features of the HR simulation. Here, 6-hourly model outputs of atmospheric circulation including winds, specific humidity, temperature, and geopotential height at 925-, 500-, and 200-hPa pressure levels from a 20-year segment of the HR simulation are used to evaluate the springtime MCS large-scale environment over the U.S. to understand the model biases in simulating MCSs.

Song et al. (2019) identified four types of synoptic environments that support the development of MCSs east of the Rocky Mountains during springtime. These environments are associated with frontal systems that provide a lifting mechanism and an enhanced Great Plains low-level jet (GPLLJ) that provides anomalous moisture for convection. During summer, MCSs often develop in the presence of

high-pressure systems over North America that suppress convection, so smaller-scale dynamical and/or thermodynamic perturbations are needed to initiate MCSs. Summer MCSs are, therefore inherently less predictable because large-scale circulation plays a less important role in their development. The analysis reported here focuses on springtime to elucidate the role of large-scale circulation biases on simulating MCSs.

To determine how well the four types of large-scale environments favorable for springtime MCSs are simulated by the model, a similarity metric is used to determine how closely the atmospheric circulation of each 6-hour snapshot from the 20-year segment of E3SM HR simulation resembles each of the four observed patterns of favorable large-scale environments. This allows us to quantify the frequency of occurrence of each type of favorable MCS environment in the simulation. Comparison of the frequency of occurrence, as well as the spatial pattern of the favorable MCS environment in the simulation and observation based on the North American Regional Reanalysis (NARR) (Mesinger et al. 2006), provides an indication of the contribution of large-scale circulation biases to the biases in modeling MCS frequency and characteristics. The similarity metric can also be designed to attribute the biases in the frequency of occurrence of the favorable MCS environments in the model to biases in simulating the winds and moisture fields of the favorable environments to gain some insights on the sources of the large-scale circulation biases.

3.0 Results

Figure 1 shows the four types of large-scale environments determined by Song et al. (2019) to be favorable for springtime (March-April-May) MCSs initiated near the foothills of the Rocky Mountains. Type-1 and Type-3 are associated with frontal systems featuring an upper-level trough upstream of the MCS initiation region, promoting upward motion for convection. The main difference between Type-1 and Type-3 is the more southward location of the upper-level trough in Type-3, so MCSs developed under the Type-3 environment are more concentrated over the Southern Great Plains than Type-1. Type-2 and Type-4 feature the GPLLJ transporting anomalous moisture to the Great Plains, providing a favorable thermodynamic environment for convection. Besides the GPLLJ, Type-2 also features an upper-level anticyclone over the Great Plains, so upward motion and MCSs are favored to develop near the western boundary of the Great Plains. Type-4 includes an upper-level cyclone to the west and an anticyclone to the east of the Southern Great Plains, which favor upward motion and MCS initiation in the Southern Great Plains.

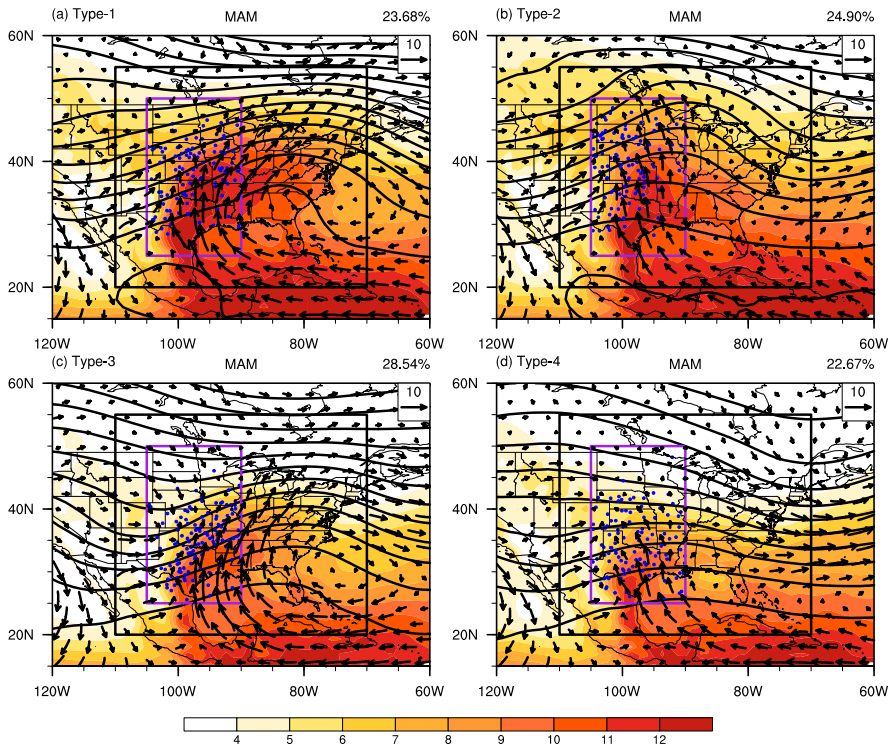

Figure 1. The four types of observed large-scale environments favorable for springtime MCS initiation near the foothills of the Rocky Mountains marked by the purple boxes. The locations of MCS initiation are marked by the blue dots inside the purple box. Black contours are 500-hPa geopotential height (gpm). Vectors are the 925-hPa winds (m s^{-1}), and shadings are the 925-hPa specific humidity (g kg^{-1}). All variables are based on the NARR data set.

A similarity metric is used to identify 6-hour snapshots of the simulated large-scale circulation that resemble the favorable large-scale environments shown in Figure 1. The mean simulated large-scale environments in the E3SM HR simulation associated with the favorable environments of Type-1 to Type-4 are shown in Figure 2. Comparison of the circulation patterns in Figure 1 and Figure 2 shows that the HR simulation is able to capture the four types of observed large-scale environments favorable for springtime MCSs. Compared to observations, the upper-level trough in Type-1 and Type-3 in the simulation is weaker, and in Type-2 and Type-4, the GPLLJ does not penetrate as deep into the Northern Great Plains in the simulation. Despite these minor differences, the observed circulation patterns supporting springtime MCS development are well simulated by the model.

Since a threshold is used in the similarity metric to select 6-hour snapshots in the simulation with atmospheric circulation resembling the observed favorable MCS large-scale environment, the spatial patterns in Figure 1 and Figure 2 are expected to be very similar by design. An important question is how often the model simulates the MCS favorable environments in the 20-year segment compared to how often such environments occur in the observations. Table 1 shows that the model simulates a significantly lower frequency for all four types of favorable large-scale environments, with larger biases for Type-1 and Type-2. Overall, favorable MCS environments occur only 18% as often as in the simulation compared to NARR. This suggests an

important role of the large-scale circulation biases in the lower frequency of MCSs simulated by the model compared to observations, as noted in the second quarter metric report.

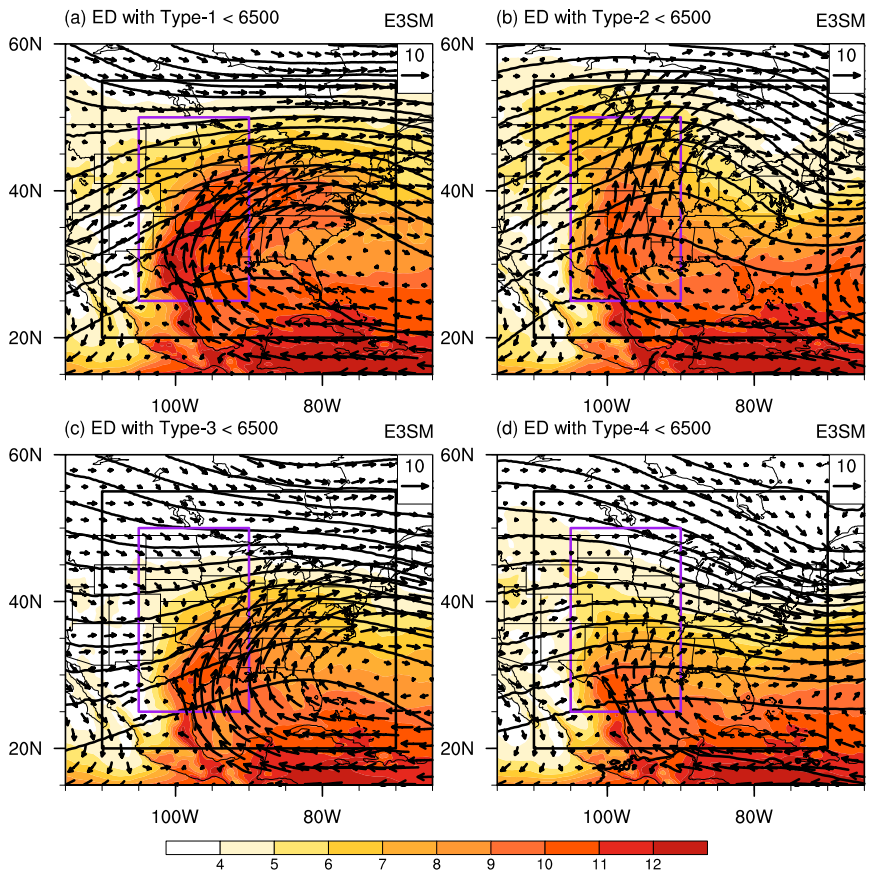

Figure 2. Similar to Figure 1, but for the mean large-scale environments from the E3SM HR simulation associated with the four types of observed large-scale environment favorable for springtime MCS development shown in Figure 1.

With the similarity metric designed to account for the mean bias in the winds and moisture, their impact on the biases in the frequency of occurrence of the favorable environment in the simulation can be assessed. Table 1 summarizes the frequency of occurrences in E3SM HR when the bias of U, V, and Q is accounted for individually. Larger increases in the occurrence frequency indicate a larger impact of the wind or moisture bias. Results show that the zonal wind (U) bias has the largest impact on the underprediction of favorable environment by the model, with the meridional wind (V) bias also contributing importantly. The wind biases have larger effects on Type-3 and Type-4, while the moisture (Q) bias also has an important effect on Type-4. With the additional number of occurrences when the bias of U, V, and Q is accounted for individually, E3SM HR can produce on average 194.5 occurrences of favorable large-scale environment per season, comparable to the 193.6 occurrences from NARR, suggesting that the linear decomposition framework of attributing model biases to U, V, and Q works quite well.

Table 1. Average number of occurrences per season for each type of favorable MCS large-scale environment and the total based on 6-hourly snapshots from NARR and the E3SM HR simulation. By accounting for the model biases in the zonal (U) and meridional (V) winds and specific humidity (Q), the occurrences of the MCS-favorable environment are also shown as E3SM HR (U), E3SM HR (V), and E3SM HR (Q), respectively.

Data	Type-1	Type-2	Type-3	Type-4	Total
NARR	55.2	31.9	40.0	57.5	193.6
E3SM HR	5.2	3.0	9.2	15.6	34.0
E3SM HR (U)	15.5	7.1	22.4	27.1	72.1
E3SM HR (V)	8.6	4.7	18.0	28.9	60.2
E3SM HR (Q)	4.4	4.7	6.2	12.9	28.2

To understand how the wind and moisture biases reduce the frequency of occurrence of the favorable MCS environments, Figure 3 shows the lower- and upper-level wind biases and the low-level moisture bias during springtime. Dry biases of up to ~2 g kg^{-1} are evident across the central and eastern U.S., with larger biases concentrated in the Southern Great Plains. Wind biases featuring stronger northwesterly flow at 925 hPa and an equatorward shift of the westerly winds at 200 hPa are obvious in the simulation. The latter indicates an equatorward bias of the upper-level jet, which is a prominent feature observed over the Southern Great Plains during spring. The low-level moisture bias is partly related to the 925-hPa wind bias that reduces the transport of moisture by the GPLLJ from the Gulf of Mexico to the Southern Great Plains. An equatorward bias of the upper-level jet and GPLLJ would have larger impacts on Type-3 and Type-4, both of which feature an upper-level trough west of the Southern Great Plains that favors upward motion and convection in that region.

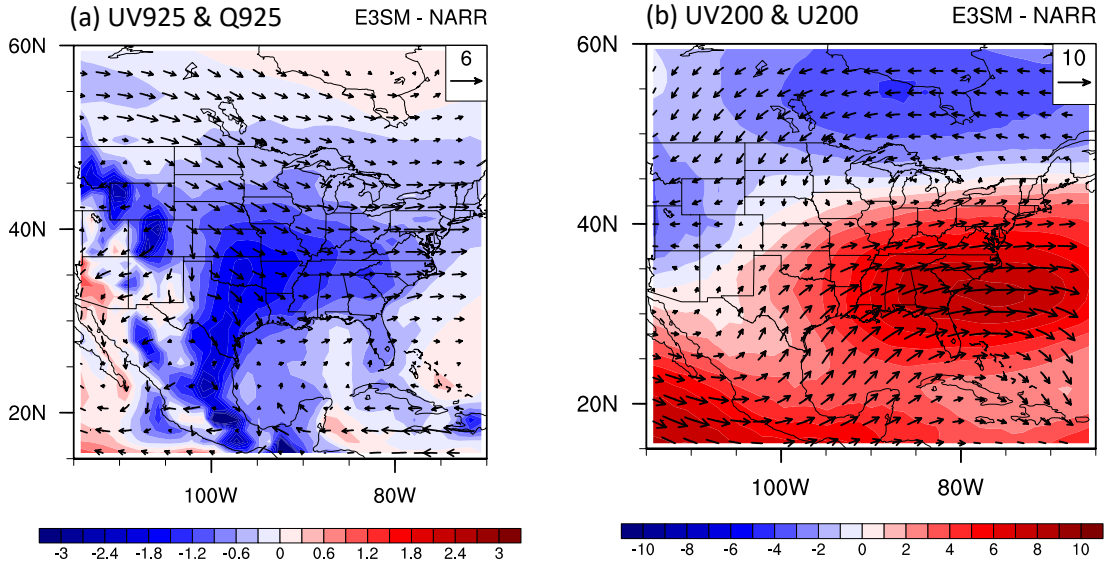

Figure 3. Biases in (a) winds vector (m s-1) and specific humidity (g kg-1, color contour) at 925 hPa, and (b) wind vector and wind speed (color contour) at 200 hPa comparing E3SM HR to NARR in the U.S.

The lower level winds in the central and eastern U.S. are strongly influenced by the North Atlantic subtropical high (NASH). Figure 4 shows the climatological geopotential height at 925 hPa in the European Center for Medium-Range Forecast Reanalysis 5 (ERA5)

(https://www.ecmwf.int/en/forecasts/datasets/reanalysis-datasets/era5) and the difference between the model simulation and ERA5. The NASH in E3SM HR is biased equatorward relative to ERA5, which is consistent with the 925-hPa wind bias in the Great Plains (Figure 3).

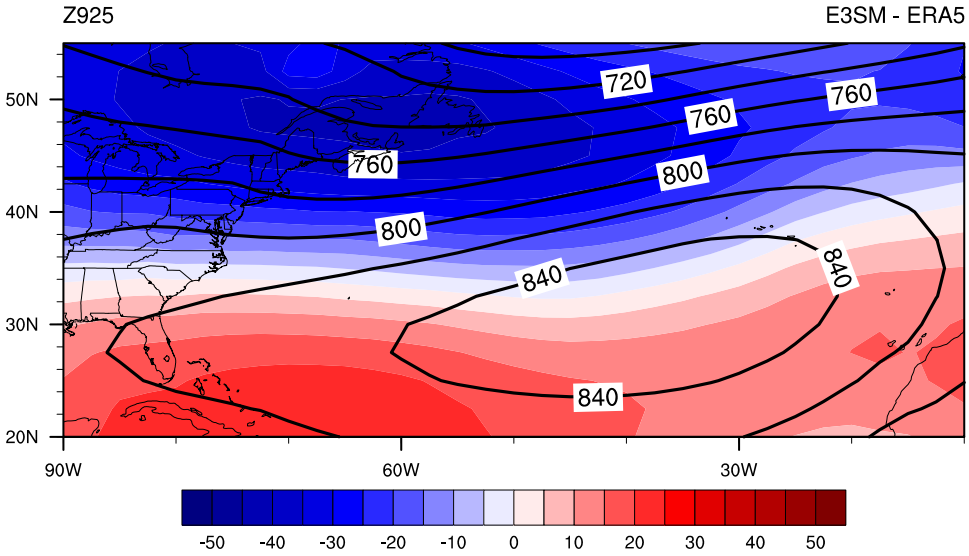

Figure 4. Climatological (contours) geopotential height (gpm) at 925 hPa from ERA5 and the difference (shading) between E3SM HR and ERA5.

In summary, notable biases in the large-scale atmospheric circulation have been identified in the E3SM HR simulation. These biases include an equatorward shift of the NASH, which has an important influence on the low-level winds that transport copious moisture from the Gulf of Mexico to the central U.S. (Helfand and Schubert 1995) to provide a favorable thermodynamic environment for MCS development in the Great Plains. An equatorward shift of the upper-level jet is also evident, which corresponds to reduced baroclinic waves in the model. As the observed divergent left exit region of the upper-level jet located over the Southern Great Plains promotes upward motion (Wang and Chen 2009), a biased location of the upper-level jet can significantly reduce the dynamical forcing for MCS development in the simulation.

Quantitative analysis of four types of favorable MCS large-scale environments in the simulation and observations supports these interpretations. Results show that the model simulates a much lower frequency of occurrence of the favorable MCS environment that is only 18% of that in the observation during springtime. Decomposing the model biases into the contributions by model biases in winds and moisture demonstrates that the wind bias has a significantly larger effect than the moisture bias on the MCS environment simulated by the model. The model large-scale circulation biases have larger impacts on the large-scale environments that favor MCSs over the Southern Great Plains during spring. Large-scale wind biases in the mid-latitudes may ultimately be linked to tropical and high-latitude biases. For example, an equatorward shift in the NASH may be related to the strength of the Hadley circulation that determines the strength and location of the NASH. Biases in the land-ocean thermal contrast may also influence the NASH, but such biases are more likely to influence the east-west location rather than the equatorward displacement of the NASH. Biases in the upper-level jet may be related to the

meridional temperature gradient, which may originate from biases in tropical convection that influence the upper tropospheric temperature in the tropics, and/or high-latitude biases such as sea ice cover in the polar region. Caldwell et al. (2019) show that arctic sea ice extent is too low in E3SM HR compared to observations, which may be symptomatic of arctic warm biases that reduce the meridional temperature gradient.

The analysis presented in this report underscores the importance of understanding model biases in the large-scale circulation, which demonstrably contributes to model biases in simulating MCSs. Arguably, the large-scale circulation biases in coupled simulations may be intimately related to limitations in convection and cloud parameterizations in the atmosphere models, making it difficult to disentangle the two. Despite this challenge, some progress can be made in addressing MCS biases in models through approaches such as the Cloud-Associated Parameterization Testbed (CAPT) framework (e.g., Ma et al. 2014) where initialized forecasts can be used to isolate the impact of model parameterizations on biases of different MCS characteristics.

The methods of analysis presented in this report on the MCS large-scale environments and those presented on MCS tracking in the second quarter metric report provide an important foundation for evaluating and understanding models' ability to simulate MCSs, which contribute significantly to the regional and global water cycle. Feng et al. (2016) revealed increases in MCS lifetime and extreme precipitation over the U.S. in the past 35 years. Prein et al. (2017) found substantial increases in MCS-like precipitation in the future based on convection-permitting regional simulations. These studies motivate the need to investigate how MCSs may change in the future using multi-model simulations. MCS tracking is possible in model simulations with grid spacing of 50 km or less, so it can be applied to simulations such as those in the HighResMIP archive to investigate how MCSs may change with warming. As part of HighResMIP, the E3SM HR configuration will be used to simulate the historical and future climates between 1950 and 2050 to support analysis of future changes of MCSs through MCS tracking. However, MCS tracking is not possible for low-resolution simulations because MCS features cannot be robustly defined at low resolution. For low-resolution simulations such as all of the CMIP6 Diagnosis, Evaluation, and Characterization of Klima (DECK) simulations (Eyring et al. 2016), MCS large-scale environments such as those discussed in this report can be analyzed in present-day and future climate simulations to provide important insights on how MCSs may respond to warming in the future.

4.0 References

Caldwell, PM, A Mametjanov, Q Tang, LP Van Roekel, J-C Golaz, W Lin, DC Bader, ND Keen, Y Feng, R Jacob, ME Maltrud, AF Roberts, MA Taylor, M Veneziani, H Wang, JD Wolfe, K Balaguru, P Cameron-Smith, L Dong, SA Klein, LR Leung, H-Y Li, Q Li, X Liu, RB Neale, M Pinheiro, Y Qian, PA Ullrich, S Xie, Y Yang, Y Zhang, K Zhang, and T Zhou. 2019. "The DOE E3SM coupled model version 1: Description and results at high resolution." *Journal of Advances in Modeling Earth Systems* 11(12): 4095−4146, https://doi.org/10.1029/2019MS001870

Eyring, V, S Bony, GA Meehl, CA Senior, B Stevens, RJ Stouffer, and KE Taylor. 2016. "Overview of the Coupled Model Intercomparison Project Phase 6 (CMIP6) experimental design and organization." *Geoscientific Model Development* 9(5): 1937–1958, https://doi.org/10.5194/gmd-9-1937-2016

Feng, Z, LR Leung, RA Houze, S Hagos, J Hardin, Q Yang, B Han, and J Fan. 2018. "Structure and Evolution of Mesoscale Convective Systems: Sensitivity to Cloud Microphysics in Convection-Permitting Simulations over the United States." *Journal of Advances in Modeling Earth Systems* 10(7): 1470−1494, https://doi.org/10.1029/2018MS001305

Feng, Z, RA Houze, LR Leung, F Song, JC Hardin, J Wang, WI Gustafson, and CR Homeyer. 2019. "Spatiotemporal Characteristics and Large-Scale Environments of Mesoscale Convective Systems East of the Rocky Mountains." *Journal of Climate* 32(21): 7303–7328, https://doi.org/10.1175/JCLI-D-19-0137.1

Haarsma, RJ, MJ Roberts, PL Vidale, CA Senior, A Bellucci, Q Bao, P Chang, S Corti, NS Fuckar, V Guemas, J von Hardenberg, W Hazeleger, C Kodama, T Koenigk, LR Leung, J Lu, J-J Luo, J Mao, MS Mizielinski, R Mizuta, P Nobre, M Satoh, E Scoccimarro, T Semmler, J Small, and J-S von Storch. 2016. "High Resolution Model Intercomparison Project (HighResMIP v1.0) for CMIP6." *Geoscientific Model Development* 9(11): 4185−4208, https://doi.org/10.5194/gmd-9-4185-2016

Haberlie, AM, and WS Ashley. 2019. "A Radar-Based Climatology of Mesoscale Convective Systems in the United States." *Journal of Climate* 32(5): 1591−1606, https://doi.org/10.1175/JCLI-D-18-0559.1

Helfand, MH, and SD Schubert. 1995. "Climatology of the simulated Great Plains low-level jet and its contribution to the continental moisture budget of the United States." *Journal of Clim*ate 8(4): 784−806, https://doi.org/10.1175/1520-0442(1995)008<0784:COTSGP>2.0.CO;2

Houze, RA. 2004. "Mesoscale convective systems." *Review of Geophysics* 42(4): RG4003, https://doi.org/10.1029/2004RG000150

Houze, RA. 2018. "100 years of research on mesoscale convective systems." *Meteorological Monographs* 59: 17.1–17.54. https://doi.org/10.1175/AMSMONOGRAPHS-D-18-0001.1

Ma, H-Y, S Xie, SA Klein, KD Williams, JS Boyle, S Bony, H Douville, S Fermepin, B Medeiros, S Tyteca, M Watanabe, and D Williamson. 2014. "On the correspondence between mean forecast errors and climate errors in CMIP5 models." *Journal of Climate* 27(4): 1781−1798, https://doi.org/10.1175/JCLI-D-13-00474.1

Prein, AF, R Rasmussen, K Ikeda, C Liu, MP Clark, and GJ Holland. 2017. "The future intensification of hourly precipitation extremes." *Nature Climate Change* 7: 48−52, https://doi.org/10.1038/nclimate3168

Song, F, Z Feng, LR Leung, RA Houze Jr, J Wang, J Hardin, and CR Homeyer. 2019. "Contrasting Spring and Summer Large-Scale Environments Associated with Mesoscale Convective Systems over the U.S. Great Plains." *Journal of Climate 32*(20): 6749−6767, https://doi.org/10.1175/JCLI-D-18-0839.1

Stevenson, SN, and RS Schumacher. 2014. “A 10-Year Survey of Extreme Rainfall Events in the Central and Eastern United States Using Gridded Multisensor Precipitation Analyses.” *Monthly Weather Review* 142(9): 3147−3162, https://doi.org/10.1175/MWR-D-13-00345.1

Wang, SY, and TC Chen,.2009. “The late spring maximum of rainfall over the U.S. central plains and the role of the low-level jet.” *Journal of Climate* 22(17): 4696−4709, https://doi.org/10.1175/2009.JCL12719.1

U.S. DEPARTMENT OF
ENERGY

Office of Science